NANO LETTERS

2006
Vol. 6, No. 10
2273−2278

Synthesis and Electrical Characterization of Silver Nanobeams

Benjamin J. Wiley,[†] Zenghui Wang,[‡] Jiang Wei,[‡] Yadong Yin,[||] David H. Cobden,[‡] and Younan Xia*[,§]

Departments of Chemical Engineering, Physics, and Chemistry, University of Washington, Seattle, Washington 98195, and The Molecular Foundry, Lawrence Berkeley National Laboratory, Berkeley, California 94720

Received July 21, 2006; Revised Manuscript Received August 30, 2006

ABSTRACT

By slowing the rate of atomic addition to singly twinned seeds, we have grown silver nanobeams with lengths of 3–30 μm, widths ranging from 17 to 70 nm, and a width to thickness ratio of 1.4. The well-defined dimensions, smooth surface, and crystallinity of nanobeams make them promising candidates for studying the effects of size on electron transport. With a simple method that allows rapid characterization of single nanobeams, we find that even the thinnest nanobeams largely retain the low resistivity of bulk silver. Nanobeams can support remarkably high current densities of up to 2.6×10^8 A cm^{-2} before the conduction path is broken by the formation of a nanogap.

A central theme of nanotechnology research is discovering and developing methods of growing useful nanoscale objects, or nanostructures, from their constituent atoms.[1,2] In synthesizing a nanostructure for a particular application, it is not only important to consider its intrinsic material properties but also to control its size and shape. For example, nanoscale silver spheres, cubes, triangular plates, and bipyramids all exhibit distinct colors because conduction electrons collectively oscillate at different resonant frequencies in each shape, and thus cause light of different frequencies to be scattered or absorbed.[3] One-dimensional nanostructures of silver are promising nanoscale conduits for electricity or heat because bulk silver has the highest electrical and thermal conductivity of any metal.[4] It is therefore important to determine down to what scale individual nanostructures of silver retain the excellent properties of the bulk material.

In this letter, we investigate the electrical properties of a new type of nanostructure, the silver nanobeam. Silver nanobeams are so named because they have a cross-sectional aspect ratio similar to that of a beam of wood. They differ from previously synthesized pentagonal silver nanowires in their dimensions, internal structure, and cross section. Like pentagonal nanowires, they grow in a direction parallel to a twin plane. Despite their small cross sections, nanobeams largely retain the low resistivity of bulk silver and can support current densities of up to 1.4×10^8 A cm^{-2} before a nanogap forms to break the conduction path.

Silver is isotropic with a face-centered cubic (fcc) crystal structure, but silver atoms can nonetheless be made to assemble in solution to form anisotropic nanostructures of different shapes by controlling (1) the presence of twin defects in the seeds from which they grow and (2) the rate of atomic addition.[5] In the initial stages of a polyol synthesis, in which ethylene glycol (EG) serves as both solvent and reducing agent, the reduced silver atoms agglomerate to form nuclei of fluctuating structure.[6] Most nuclei incorporate twin boundary defects because such defects enable a lower surface energy.[7] As nuclei grow, fluctuations cease, and a distribution of single-crystal, singly twinned, and multiply twinned seeds form, with the 5-fold twinned decahedron being the lowest-energy and most abundant morphology.

The key to obtaining silver nanostructures of one specific shape to the exclusion of others is controlling the crystallinity of seeds formed in the nucleation step. Addition of a corrosive anion such as chloride selectively etches twinned seeds and enables the production of pure single-crystal seeds that grow to form nanocubes whose level of corner truncation can be controlled by the rate of atomic addition.[8,9] Conversely, if oxidative etching is prevented through the removal of oxygen from the reaction, then the product is dominated by pentagonal nanowires that grow from decahedron seeds.[10] If a less corrosive anion such as bromide is substituted for chloride, then there is still adequate etching to eliminate the multiply twinned seeds, but seeds with a single twin remain intact.[11] These single twinned seeds grow to form right bipyramids in 3−5 h. By decreasing the rate of atomic addition to these same single twinned seeds, we found that we could grow silver nanobeams.

* Corresponding author. E-mail: xia@chem.washington.edu.
[†] Department of Chemical Engineering.
[‡] Department of Physics.
[§] Department of Chemistry.
[||] Lawrence Berkeley National Laboratory.

10.1021/nl061705n CCC: $33.50
Published on Web 09/15/2006

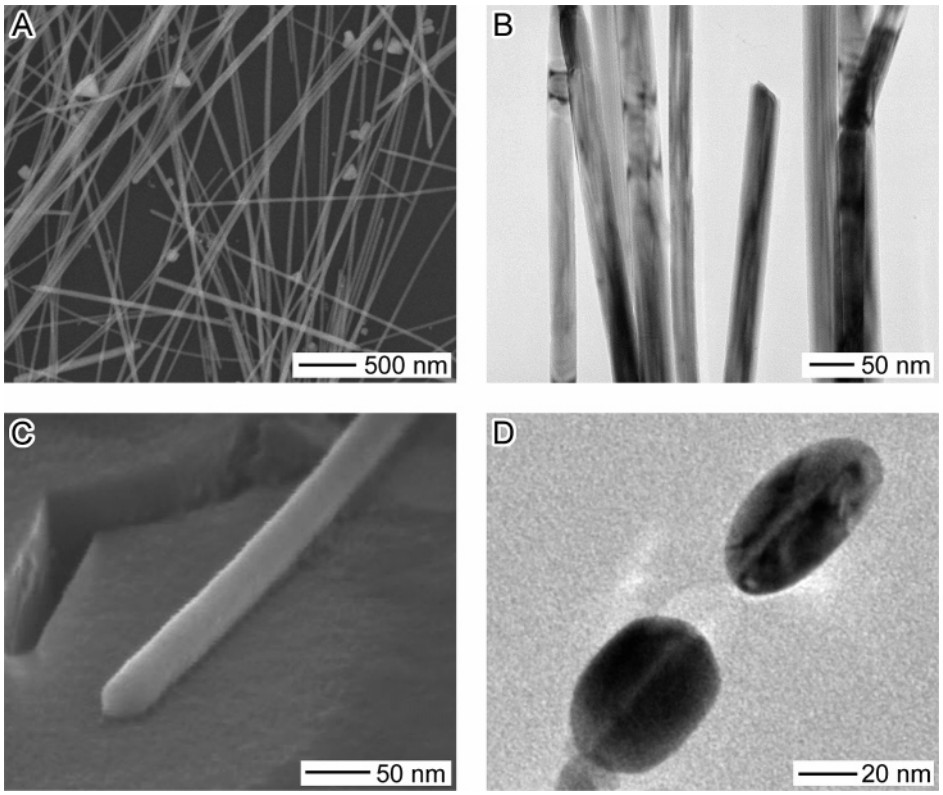

Figure 1. (A) SEM and (B) TEM images of silver nanobeams. (C) SEM image of a nanobeam tilted at 65° relative to the electron beam, where its rounded profile is visible (the scale bar only applies to the horizontal axis). (D) TEM image of a microtomed sample of silver nanobeams showing their cross-sectional profile. This image suggests that the nanobeam is bisected by a twin plane parallel to the base.

To synthesize nanobeams, two EG solutions, one containing 96 mg $AgNO_3$ in 3 mL EG, the other containing 96 mg poly(vinyl pyrrolidone) (PVP) and 0.034 mg NaBr in 3 mL EG, were added dropwise via a two-channel syringe pump into 5 mL of EG heated in an oil bath at 148 °C. Compared to the synthesis of right bipyramids, the concentration of $AgNO_3$ and PVP was doubled and the temperature was lowered by 12 °C. Although the concentration of silver precursor was doubled, the lower reaction temperature resulted in a much slower reduction rate. After injection, the reaction solution initially appeared bright yellow, indicating the formation of small (<20 nm) spherical nanoparticles, but the solution gradually turned clear by 1 h because of oxidative etching.[8] By about 20 h, a light yellow tint returned to the reaction solution, and this color became a translucent, silvery gray by 24 h as the seeds grew to form nanobeams.

Figure 1A is a scanning electron microscopy (SEM) image of the silver nanobeams produced after 24 h. Their widths ranged from about 17 to 70 nm; about 85% had widths less than 40 nm, and 40% less than 30 nm. On the basis of this image and others, we estimate that 95% of the nanobeams were over 3 μm long, approximately 60% were over 10 μm long, and 10% were over 30 μm long. Usually those nanobeams with greater lengths also had greater widths so that nanobeams longer than 30 μm had widths of at least 40 nm. Figure 1B shows a transmission electron microscopy (TEM) image, in which nanobeams displayed striations of contrast quite distinct from the 2-fold contrast characteristic of pentagonal nanowires.[12] This contrast may result from slight bending and/or twisting of the nanobeams. To view the cross section of the nanobeams, we oriented the sample normal at 65° to the electron beam in an SEM. Figure 1C shows that at this viewing angle a nanobeam appears to have a somewhat rounded profile. To obtain a clearer picture of the cross section and internal structure of the nanobeams, we suspended them in epoxy and microtomed 100 nm thick slices for viewing under TEM. The cross sections of two nanobeams can be seen in Figure 1D. Both appear to be bisected by a single twin plane, suggesting that the nanobeams grew from singly twinned seeds. To analyze the cross-sectional dimensions, we considered the nanobeam in the lower left of this image because it appears to be more closely aligned with the electron beam. This cross section is 38 nm wide and 27 nm thick; hence, the width to thickness ratio W/T is 1.4. If 17 nm wide nanobeams have similar dimensions, then they will only be 12 nm thick.

At present, we do not completely understand the growth mechanism of silver nanobeams. However, a slow reduction rate has previously been found to facilitate the anisotropic growth of single-crystal seeds in the polyol synthesis of platinum nanowires.[13] This anisotropic growth may result from the fact that, when there is a small driving force for atomic addition, atoms add only to the most energetically favorably sites on a nanostructure. In the case of single twinned seeds of silver, defects at the twin boundary provide a favorable site for atomic addition and the nucleation of new atomic layers.[14] If such defects were greater in number

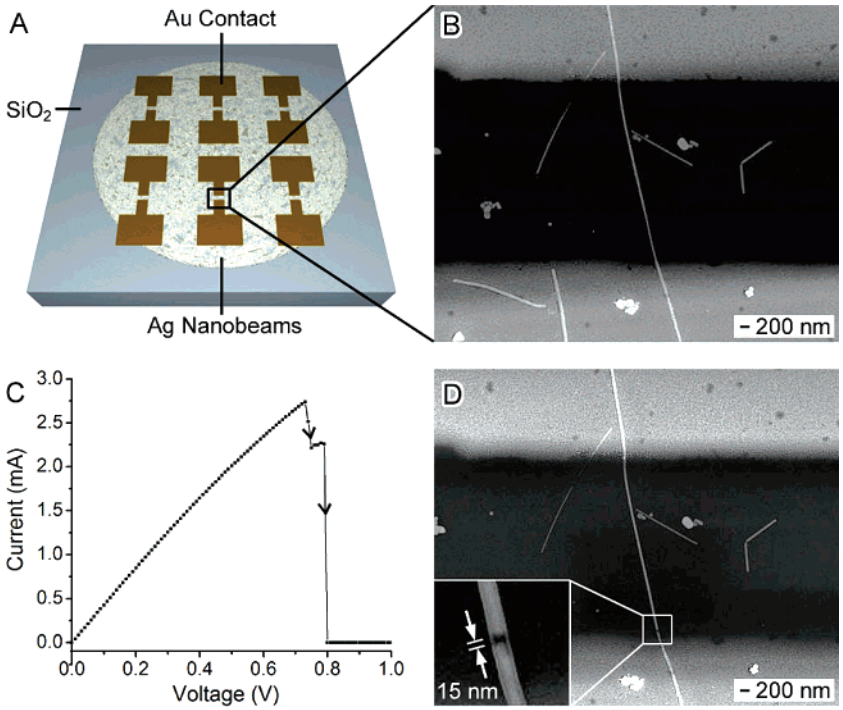

Figure 2. (A) Gold contacts were evaporated onto Ag Nanobeams to measure their electrical properties. (B) SEM image of a single nanobeam 45 nm wide and 30 nm high spanning the gap beneath the gold contacts. (C) The nanobeam could support a current up to 2.7 mA at room temperature before gap formation caused the current to drop to zero (the ramp speed was 10 mV/s). (D) SEM image of the nanobeam after testing for the maximum current it could support. The inset is a magnified image of the 15 nm gap that formed as a result of the large current density. The linear features remaining at the sides of the gap are probably residual polymer.

on one side of the seed, then the greater rate of atomic layer generation on that side could result in the anisotropic growth of nanobeams.

To make electrical contact with a single nanobeam, an aqueous suspension of nanobeams was dried on an oxidized silicon substrate, after which gold was evaporated through a shadow mask to make gold contacts (see Figure 2A). Figure 2B shows an SEM image of a nanobeam spanning gold contacts separated by 4 μm. The nanobeam was measured to be 45 nm wide from SEM, and 30 nm thick by atomic force microscopy (AFM), giving $W/T = 1.5$, consistent with the results of TEM analysis. At low bias, this nanobeam had a stable ohmic resistance of 248 Ω. As the bias was increased at a rate of 10 mV/s, failure occurred at a current of about 2.7 mA, as shown in Figure 2C. This corresponds to a current density of 2.6×10^8 A cm^{-2}. Failure occurred by formation of a gap about 15 nm wide in the nanobeam at the edge of one of the contacts, as can be discerned in the SEM images in Figure 2D. With careful control of the current during the electromigration process that forms the gap, we expect to be able to form considerably smaller gaps. The formation of such gaps suggests this procedure as a simple way of fabricating nanoscale electrodes separated by a few nanometers that, unlike previous methods, completely circumvents the need for lithography.[15]

This initial contacting technique had two drawbacks. One was the low probability of obtaining a gap spanned by a single nanobeam. The second was that most nanobeams smaller that 40 nm in width exhibited small breaks at the edges of one or both contacts before any bias was applied, as illustrated in Figure 3A. The origin of the breaks is unclear, but we speculate that they are related to silver/gold alloying and the high surface mobility of silver atoms. They were also found to occur when the nanobeams are deposited on top of preformed gold contacts. However, we succeeded in eliminating the breaks by switching to the following procedure: (1) evaporating the gold contacts on the SiO_2 and immersing in a 1 mM 1-octadecanethiol (ODT) solution to coat the gold with an ODT monolayer; (2) drying droplets of nanobeam suspension on top of these contacts and again submerging the device in ODT solution to coat the silver; and (3) annealing the nanobeams individually to the gold contacts with a focused electron beam. This procedure, illustrated in Figure 3B, has the additional advantage that it eliminates the need to find gaps in gold spanned by a single nanobeam. Instead, any one out of several nanobeams spanning a given gap can be selected for annealing and electrical characterization.

Figure 3C shows a 27 nm wide and 19 nm thick nanobeam ($W/T = 1.4$) spanning gold contacts separated by 1.5 μm. The initial resistance was 2.5 MΩ (Figure 3D), a high value that can be attributed to the presence of an insulating ODT monolayer between the gold and the nanobeam. To obtain metal-to-metal contact, we focused the electron beam (130 μA, 20 kV) for about 1 min at points on the nanobeam where it lay on the gold. Figure 3E shows that the electron beam was focused on the very ends, resulting in slight deformation as can be seen in the inset magnified images. After this process the resistance decreased by 4 orders of magnitude to 223 Ω.

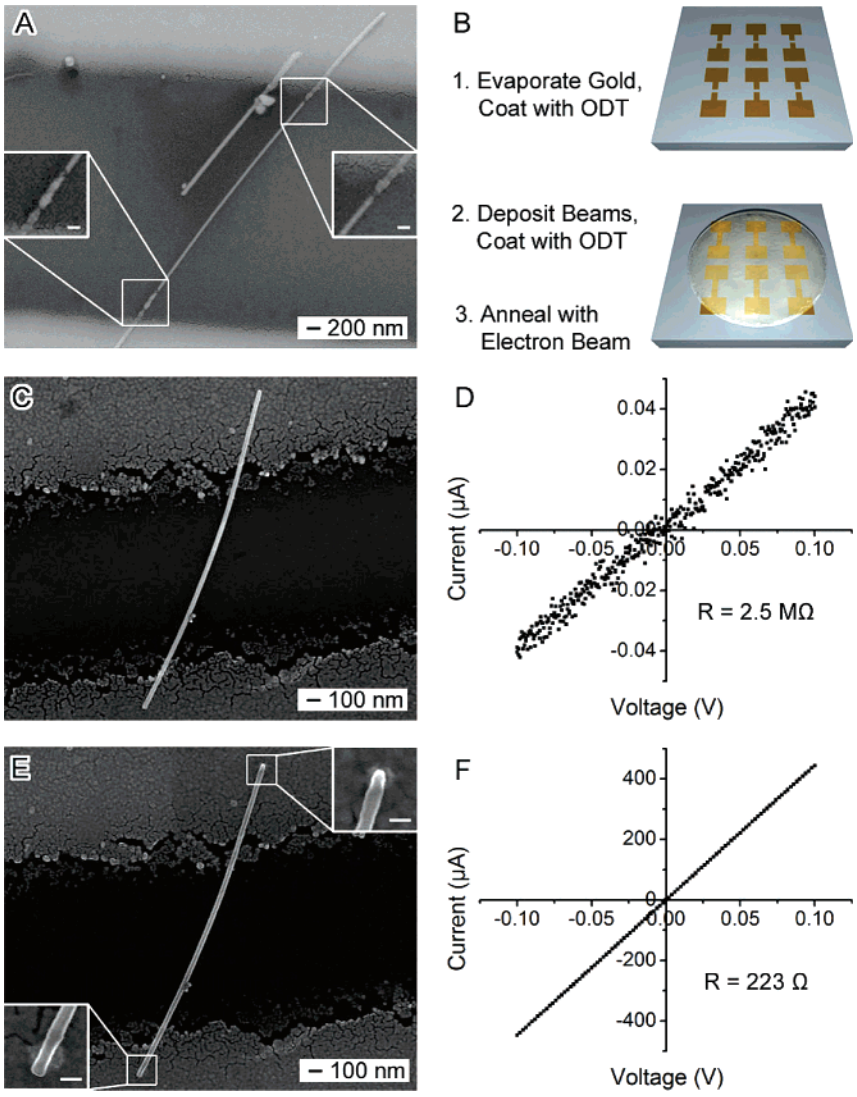

Figure 3. (A) SEM image illustrating the breakage that occurred in a 35 nm wide nanobeam before a bias was applied (inset scale bar = 100 nm). (B) Premature breakage was prevented by covering the gold contacts with an ODT monolayer before depositing nanobeams on top and annealing them to the gold with an electron beam. (C) SEM image of a single nanobeam 27 nm wide and 19 nm high spanning the gap across the gold contacts. (D) The ODT monolayer on the gold insulated the nanobeams, giving an initial resistance of 2.5 MΩ. (E) SEM of the same nanobeam after annealing the ends to the contacts with a focused electron beam, with insets showing the resultant deformation (scale bar = 50 nm). (F) The resistance decreased by about 10 000 times after annealing.

The key properties of these metal nanobeams at room temperature are their resistivity and current-carrying ability. To investigate these, we measured a collection of nanobeams with different lengths L and widths W (with $W/T \approx 1.4$ for all). The effective resistivity, ρ, of a uniform metal film or wire will be higher than the bulk value, ρ_0, because of surface scattering. If we take wires of a given cross-sectional shape and consider reducing the cross-sectional area $A \equiv a^2$, then the correction to ρ should initially be linear in the surface to volume ratio, a^{-1}, that is, $\rho = \rho_0(1 + \lambda/a)$, where λ is a characteristic length scale and $\lambda/a << 1$.[16] Such an expression has provided a good fit in a wide range of thin film and wire measurements even when a is comparable with λ, although different expressions are needed in the limit $\lambda/a >> 1$.[17] The scale λ is set by the bulk mean free path l, the shape, and the details of the surface scattering. In addition to the bulk resistance of the nanobeam, we anticipate a contact resistance, R_c. Assuming for simplicity that R_c is the same for every device, and putting $A \approx \pi WT/4 \approx 0.56W^2$ and $a = A^{1/2} \approx 0.75W$ for the nanobeams, we obtain

$$R - R_c \approx \rho \frac{L}{A} \approx \rho_0 \frac{L}{0.56W^2}\left(1 + \frac{\lambda}{0.75W}\right) \qquad (1)$$

To see how well this describes the nanobeams, we plot values of R against values of the expression on the right-hand side of eq 1 calculated using the bulk value of $\rho_0 = 1.6\ \mu\Omega$ cm for silver and a value of λ that was adjusted to give the best fit to a straight line of slope unity. The result is shown in Figure 4A, with $\lambda = 15$ nm and a best fit straight line giving $R_c = 164\ \Omega$. We deduce that the data is consistent with eq 1. The scatter about the straight line could be explained by random variations in the resistance of the

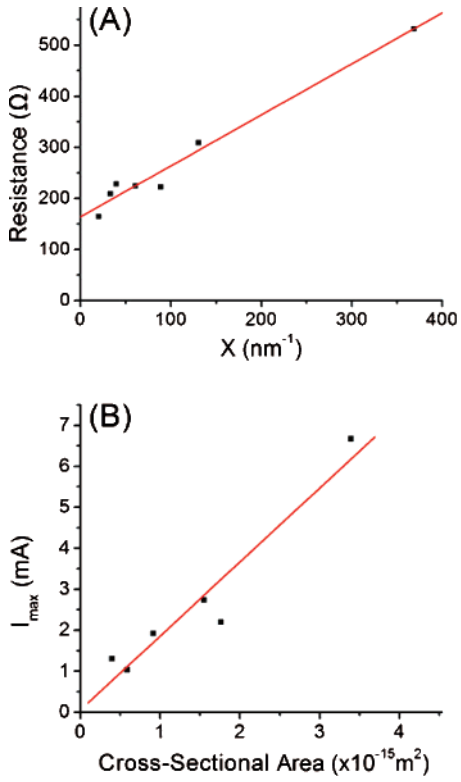

Figure 4. (A) Plot of resistance vs $X = \rho_0 \frac{L}{0.56W^2}\left(1 + \frac{\lambda}{0.75W}\right)$ for seven nanobeams using $\lambda = 15$ nm. The straight line fit has a slope of unity, and the y intercept gives a contact resistance $R_c = 164$. Here λ is a characteristic thickness at which the resistivity deviates from bulk silver, and is in principle determined by the bulk mean free path l, the shape, and the details of the surface scattering. (B) The current at failure I_{max} is roughly proportional to the cross-sectional area of the nanobeams.

contacts. Because, according to eq 1, even our thinnest nanobeams, with $W \approx 20$ nm, have a resistivity only twice that of bulk silver, it appears that the nanobeams largely retain the unparalleled electrical conductivity of the bulk material.

The resistivity correction depends on the way conduction electrons scatter from the metal surface. A semiempirical calculation for a circular wire gives $\lambda = (3/4)(1 - p)l$, where p is the fraction of surface scattering that is specular (i.e., mirror-like).[16] [Note that if surface scattering were completely specular ($p = 1$) then it would have no effect on the resistivity ($\lambda = 0$) because each electron would retain its momentum along the wire on scattering from the surface.] Substituting $\lambda = 15$ nm and the known bulk mean free path $l \approx 52$ nm, we obtain $p \approx 0.6$. This is consistent with the values of p found in transverse electron focusing experiments on polished bulk crystals of silver at 4.2 K.[18] The consistency is quite surprising considering that surface phonon scattering is insignificant at 4.2 K but is expected to diminish p in the silver nanobeams measured at room temperature.[19,20] However, we note that in support of these findings, arrays of single-crystal silver nanowires grown in polymeric templates by electrodeposition have recently been reported to exhibit almost the same low resistivity as our nanobeams.[21] To reiterate, it appears that the resistivity of silver nanobeams is as low as one could hope to achieve in uniform, smooth, defect-free silver wires.

Last, we investigated the maximum current the nanobeams can support. The current at failure, I_{max}, is plotted versus cross-sectional area A in Figure 4B. The data is consistent with $I_{max} \propto A$ with a slope representing a well-defined maximum current density of approximately 1.8×10^8 A cm^{-2}. This is comparable to the highest current densities reported for multiwalled carbon nanotubes ($\sim 10^9$ A cm^{-2}).[22,23]

In summary, silver nanobeams synthesized in solution exhibit superb electrical properties. Their resistivity remains comparable with the bulk material for thicknesses down to less than 15 nm, and their current carrying capacity is comparable to the highest reported for multiwalled carbon nanotubes. These consistent and predictable characteristics, in addition to the ease with which they can be grown and handled, make silver nanobeams a competitive option for use as electrical interconnects. Further, passage of a large current can convert nanobeams into nanoscale electrode pairs, circumventing the need for lithography. Thus, silver nanobeams serve as an excellent example of how the assembly of atoms in solution can be guided to generate useful nanostructures.

Acknowledgment. This work was supported in part by the NSF (DMR-0451788), the U.S. Army Research Laboratory and the U.S. Army Research Office under contract number 48385-PH, and a fellowship from the David and Lucile Packard Foundation. Y.X. is a Camille Dreyfus Teacher Scholar (2002−2007). B.W. thanks the UW Center for Nanotechnology for an IGERT fellowship funded by the NSF (DGE-9987620). Z.W. was supported by a fellowship from the University of Washington Initiatives Fund. This work used the Nanotech User Facility (NTUF) at the UW, a member of the National Nanotechnology Infrastructure Network (NNIN) funded by the NSF. We thank the Molecular Foundry at the Lawrence Berkeley National Laboratory for the HRTEM analysis.

Supporting Information Available: Detailed descriptions of materials and methods. This material is available free of charge via the Internet at http://pubs.acs.org.

References

(1) Whitesides, G. M.; Boncheva, M. *Proc. Natl. Acad. Sci. U.S.A.* **2002**, *99*, 4769.
(2) Xia, Y.; Yang, P.; Sun, Y.; Wu, Y.; Mayers, B.; Gates, B.; Yin, Y.; Kim, F.; Yan, H. *Adv. Mater.* **2003**, *15*, 353.
(3) Wiley, B.; Im, S.-H.; Li, Z.-Y.; McLellan, J.; Siekkinen, A.; Xia, Y. *J. Phys. Chem B* **2006**, 110, 15666.
(4) Carmon, F.; Barreau, F.; Delhaes, P.; Canet, R. *J. Phys. Lett.* **1980**, *41*, L-531.
(5) Wiley, B.; Sun, Y.; Mayers, B.; Xia, Y. *Chem.—Eur. J.* **2005**, *11*, 454.
(6) Smith, D. J.; Petford-Long, A. K.; Wallenberg, L. R.; Bovin, J. O. *Science* **1986**, *233*, 872.
(7) Ajayan, P. M.; Marks, L. D. *Phys. Rev. Lett.* **1998**, *60*, 585.
(8) Wiley, B.; Herricks, T.; Sun, Y.; Xia, Y. *Nano Lett.* **2004**, *4*, 1733.
(9) Im, S.-H.; Lee, Y. T.; Wiley, B.; Xia, Y. *Angew. Chem., Int. Ed.* **2005**, *44*, 2154.
(10) Wiley, B.; Sun, Y.; Xia, Y. *Langmuir* **2005**, *21*, 8077.
(11) Wiley, B.; Xiong, Y.; Li, Z.-Y.; Xia, Y. *Nano Lett.* **2006**, *6*, 765.
(12) Sun, Y.; Mayers, B.; Herricks, T.; Xia, Y. *Nano Lett.* **2003**, *3*, 955.

(13) Chen, J.; Herricks, T.; Geissler, M.; Xia, Y. *J. Am. Chem. Soc.* **2004**, *126*, 10854.
(14) Lofton, C.; Sigmund, W. *Adv. Funct. Mater.* **2005**, *15*, 1197.
(15) Park, H.; Lim, A. K. L.; Alivisatos, A. P.; Park, J.; McEuen, P. L. *Appl. Phys. Lett.* **1999**, *75*, 301.
(16) Dingle, R. B. *Proc. R. Soc. London, Ser. A* **1950**, *201*, 545.
(17) Sondheimer, E. H. *Adv. Phys.* **1952**, *1*, 1.
(18) Tsoi, V. S.; Bass, J.; Benistant, P. A.; van Kempen, H.; Payens, E. L. M.; Wyder, P. *J. Phys. F: Metal Phys.* **1979**, *9*, L221.
(19) Tsoi, V. S.; Bass, J.; Wyder, P. *Rev. Mod. Phys.* **1999**, *71*, 1641.
(20) Kim, S.; Suhl, H.; Schuller, I. K. *Phys. Rev. Lett.* **1997**, *78*, 332.
(21) Bid, A.; Bora, A.; Raychaudhuri, A. K. *Phys. Rev. B* **2006**, *74*, 035426.
(22) Bourlon, B.; Glattli, D. C.; Placais, B.; Berroir, J. M.; Milko, C.; Forro, L.; Bachtold, A. *Phys. Rev. Lett.* **2004**, *92*, 026804.
(23) Wei, B. Q.; Vajtai, R.; Ajayan, P. M. *App. Phys. Lett.* **2001**, *79*, 1172.

NL061705N